AoI-Inspired Collaborative Information Collection for AUV-Assisted Internet of Underwater Things

Zhengru Fang, *Graduate Student Member, IEEE*, Jingjing Wang, *Member, IEEE*, Chunxiao Jiang, *Senior Member, IEEE*, Qinyu Zhang, *Senior Member, IEEE*, and Yong Ren, *Senior Member, IEEE*

***Abstract*—In order to better explore the ocean, autonomous underwater vehicles (AUVs) have been widely applied to facilitate the information collection. However, considering the extremely large-scale deployment of sensor nodes in the Internet of Underwater Things (IoUT), a homogeneous AUV-enabled information collection system cannot support timely and reliable information collection considering the time-varying underwater environment as well as AUV's energy and mobility constraints. In this article, we propose a multi-AUV-assisted heterogeneous underwater information collection scheme for the sake of optimizing the peak Age of Information (AoI). Moreover, the limited service M/G/1 vacation queueing model is utilized to model the process of information exchange, where the optimal upper limit of the number of AUVs served in the queueing system as well the steady-state distribution of the queue length are derived. A low-complexity adaptive algorithm for adjusting the upper limit of the queuing length is also proposed. Finally, simulation results validate the effectiveness of our proposed scheme and algorithm, which outperform traditional methods in terms of the peak AoI.**

***Index Terms*—Age of Information (AoI), Internet of Underwater Things (IoUT), queueing theory, underwater information collection.**

I. Introduction

THE SMART ocean has emerged as the future goal of Internet of Underwater Things (IoUT), which requires the revolution of the present approaches of sensing and understanding the underwater world. Hence, it has an urgent need for supporting reliability-sensitive and latency-sensitive information services in a range of compelling IoUT applications, such as toxic chemical spill monitoring [1], marine search and rescue services [2], underwater intelligence gathering for military mission [3], where the timeliness of data collected is closely related to the course of these events and even the life safety of workers, which meet the trend of the smart ocean. Since Qiu *et al.* [4] introduced the concept of IoUT, there have been a various of literatures focusing their attention on improving the conventional communication performance metrics, such as throughput, transmission latency and packet delivery ratio, etc. However, few works have concerned about the timeliness of the data from being generated to being collected, which indicates the "freshness" of the data.

In traditional wireless sensor networks (WSN), this so-called 'freshness' of data can be measured by a promising metric, namely the Age of Information (AoI) [5]–[7]. Moreover, the definition of AoI is entirely different from those standard network performance metrics, such as packet delay, throughput, just to name a few. Latency is the time that packets travel from the sender to the receiver, while AoI has been used to describe the time elapsed since the last data generated from the source node is received by the destination node, which benchmarks the latency of the whole process of information collection, including the latency in the sensing process, transmission process as well as computation process, if appropriate.

However, the traditional information collection schemes and AoI-oriented optimization methods for the land-based Internet of Things (IoT) networks cannot be extended to the IoUT in virtue of the following unique characteristics of the underwater environment.

1) Many factors of uncertainty in underwater environment also affect the deployment of IoUT, such as the turbid water medium causes the uncertainty and complexity of IoT nodes' location.
2) The long propagation latency and large Doppler spread contribute to the serious multipath spread and time variation.
3) The transmission power of underwater acoustic communication is much higher than that of radio wave communication while charging or replenishing storage batteries underwater is quite complicated.

To overcome the aforementioned challenges in IoUT, based on the utilization of autonomous underwater vehicles (AUVs) and the deployment of the IoT nodes, two kinds of data acquisition schemes for IoUT networks have been proposed [8], [9]. One is based on the self-organizing of the underwater

Manuscript received July 19, 2020; revised November 9, 2020; accepted December 30, 2020. Date of publication January 5, 2021; date of current version September 23, 2021. This work was supported in part by the National Natural Science Foundation of China under Grant 62071268, and in part by the Project "The Verification Platform of Multi-Tier Coverage Communication Network for Oceans" of Peng Cheng Laboratory under Grant LZC0020. *(Corresponding author: Chunxiao Jiang.)*

Zhengru Fang and Jingjing Wang are with the Department of Electronic Engineering, Tsinghua University, Beijing 100084, China (e-mail: fangzhengru@gmail.com; chinaeephd@gmail.com).

Chunxiao Jiang is with the Tsinghua Space Center, Tsinghua University, Beijing 100084, China (e-mail: jchx@tsinghua.edu.cn).

Qinyu Zhang is with the Communication Engineering Research Center, Harbin Institute of Technology, Shenzhen 518055, China, and also with the Network and Communication Research Center, Peng Cheng Laboratory, Shenzhen 518055, China (e-mail: zqy@hit.edu.cn).

Yong Ren is with the Department of Electronic Engineering, Tsinghua University, Beijing 100084, China, and also with the Network and Communication Research Center, Peng Cheng Laboratory, Shenzhen 518055, China (e-mail: reny@tsinghua.edu.cn).

Digital Object Identifier 10.1109/JIOT.2021.3049239

IoT nodes enabled by clustering and multihop transmission schemes, which can relay real-time information to the data center yet may also lead to heavy workload in certain nodes and extra energy consumption [10]. The other one relies on flexible AUVs to collect information from underwater IoT nodes, which has gained increasing attention [11]–[13]. To elaborate a little further, Yan *et al.* [14] presented an energy-efficient information collection scheme relying on a single AUV for IoUT and designed a dynamic value-based trajectory strategy for the AUV considered. Additionally, benefiting from the cooperation of multiple AUVs, Han *et al.* [15] proposed a multi-AUV-aided information collection scheme, which was concerned about the AUV's malfunctions. In [16], the reinforcement learning algorithm was conceived by Wang *et al.* for guiding multiple AUVs information collection task in the context of a constrained continuous space. By utilizing the AUVs in IoUT, the lifetime of underwater IoT nodes can substantially extended, while it can also result in relatively high AoI because AUVs have to serve each IoT node relying on a given trajectory. Hence, it is necessary to strike a tradeoff between the energy consumption of both AUVs and IoT nodes as well as the AoI of the IoUT system.

Inspired by the above-mentioned issues, in this article, we proposed a heterogeneous multi-AUV-assisted information collection scheme, where two kinds of AUVs are used and the energy constraint of AUVs is considered. Our main contributions can be summarized as follows.

1) To the best of our knowledge, this is the first work for multi-AUV-assisted heterogeneous underwater information collection system for IoUT considering both the realistic complex underwater acoustic environment and the AUV's energy consumption, where the AUV's trajectory problem is formulated as a combinatorial optimization problem under the constraint of energy-consumption and Hamiltonian path rule.
2) A limited service M/G/1 vacation queueing model is constructed for describing and optimizing the AoI of the IoUT. Specifically, based on the probabilistic AoI metric, its optimal upper limit of the number of AUVs served in the queueing system is obtained, which makes a tradeoff between the timeliness of underwater information and the energy consumption of AUVs. Moreover, we derive the steady-state stationary distribution of the queue length and its relationship with the AoI as well as the arrival rate of AUVs. Also, a low-computational algorithm is proposed for adaptively adjusting the upper limit of the queuing length formulated.
3) Extensive simulations are conducted to evaluate the performance of information collection scheme proposed in comparison to the other single AUV or multi-AUV-aided schemes. Simulation results show that our proposed AUV-assisted information collection system and queueing mechanism reduce the peak AoI under energy constraints.

The remainder of this article is organized as follows. The related works about AUV-assisted information collection schemes for IoUT as well as AoI optimization approaches are reviewed in Section II. The system model is provided in Section III, which illustrates the heterogeneous multi-AUV-aided information collection scheme and the derivation of acoustic signal channel. We studied the derivations of peak AoI for our proposed scheme in Section IV. The details of the trajectory problem and energy-consumption are given in Section V. The limited service M/G/1 vacation queueing system and its steady stationary distribution are presented in Section VI. In Section VII, simulation results are provided for characterizing our proposed AUV-assisted information collection scheme, followed by our conclusions in Section VIII.

II. Related Work

In the literature, optimizing the AoI for ground IoT networks has been widely studied for the requirement of information freshness in IoT devices [17]–[19]. Kam *et al.* [20] analyzed the fixed and random exponential deadline in $M/M/1/2$ queueing system to quantify the degree of dissatisfaction of information "freshness," which proved that using a deadline has a better performance in $M/M/1/1$ and $M/M/1/2$ queueing system. In order to find an AoI-minimized transmission scheduling scheme, a discrete-time decision problem was formulated by Kadota *et al.* [21], then the authors proposed three low-complexity policies to minimize AoI of the broadcast wireless networks. In [22], considering a monitor collects information from the multiple independent sources, Yates and Kaul derived a general consequence for various kinds of multiple update system, such as the $M/M/1$ first-come first-served (FCFS) and last-come first-served (LCFS) queueing system. Similarly, Inoue *et al.* have studied the results of AoI evaluation under different stationary distributions, which could be utilized for a wide variety of information update single-server queues [23]. Seo and Choi [24] investigated the peak AoI closed-form expression in $D/M/1$. The metric of AoI also used in the cognitive radio system to optimize the timeliness of the status updates. In [25], the cognitive radio energy harvesting communication system is investigated from the queueing theory with the primary users. Gu *et al.* [26] considered a cognitive radio-based IoT network, which consists of primary IoT devices,and the authors proposed a status updates scheme regarding the minimization of average AoI. Considering the multiple devices coexist in sharing the networks' capacity, the competitions between different IoT nodes lead to the conflict. Therefore, Hao and Duan [27] designed a trigger mechanism of nonmonetary punishment by game theory. The primary result is that the optimization of time average AoI for data freshness is neither the throughput nor the latency. Besides, the mainstream discussions of AoI focused more on the fixed IoT nodes but ignored the mobile applications, such as the Internet of vehicles and not to mention the AUV-aided networks.

The use of the mobile vehicles in IoT system drew people's attention to the unmanned aerial vehicle (UAV), vehicles and AUV as mobile nodes to relay the information [28], [29], which improved the performance of data freshness in IoT system. For instance, Abd-Elmagid and Dhillon proposed an efficient iterative algorithm to address the issues of UAV's flight trajectory problems under the service time allocations and energy constraints [30]. Besides, the work

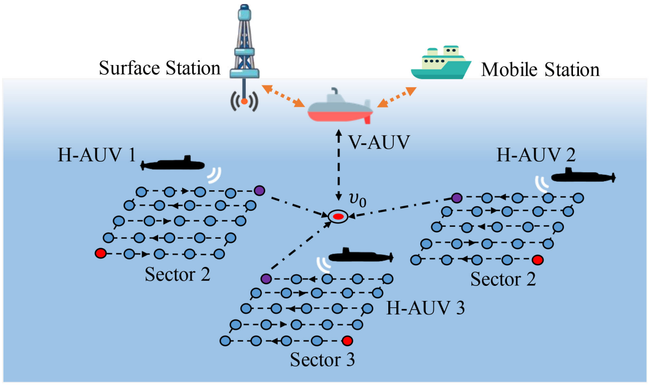

Fig. 1. Illustration of the AUV-assisted data sensing model.

in [31] considered the model of UAV trajectory planning with a min–max-AoI-optimal path scheme, which can be solved by the proposed reinforcement learning-based strategy. Furthermore, AUV-aided information collection schemes are another research hotspot for IoUT and several sophisticated schemes have been studied in literature to satisfy the requirement of IoUT. For instance, the AUV information collection scheme based on location prediction has been proposed by Han *et al.* to overcome the unbalanced energy consumption [32]. Lin *et al.* [33] investigated the paradigm of SDN technology and designed an SDN-based underwater cooperative searching strategy by using multiple AUVs. However, few references discussed the information freshness of IoUT nodes. Wang and Wu [34] designed an AUV enabled trajectory scheduling for IoUT, which has proposed an optimal schedule to minimize the total time of surfacing for information collection. Moreover, Khan *et al.* [35] designed a traversal algorithm for the improvement of the overall data freshness. Nevertheless, the proposed scheme only considered the elapsed time since IoUT nodes collected by AUV to the surface station without the consideration of the elapsed time for information stored in the nodes before being collected.

As mentioned above, the aforementioned studies did not consider the peak AoI performance for the information fresh-sensitive applications in IoUT. To address above issues, this work provided a heterogeneous multi-AUVs-aided information collection scheme, which utilized the significant metric peak AoI to avoid the information expiration. Based on the queueing theory, the closed-form solution of the peak AoI has been derived and a low-complexity adaptive algorithm for adjusting the upper limit of the queuing length is also proposed.

III. System Model

A. Multi-AUV-Aided Information Collection Scheme

As depicted in Fig. 1, a heterogeneous multi-AUV information collection scheme is proposed for IoUT including the fixed sensor nodes in the seabed and two types of AUVs, namely H-AUV and V-AUV. H-AUV is designed for collecting the information from IoUT nodes fixed in the seabed and V-AUV can receive information from H-AUVs and send them to surface station. Moreover, H-AUV moves on the 2-dimensional (2-D) plane over the seabed without surfacing, which is capable of supporting seamless coverage and long-time underwater operation for its easy deployment and maneuverability, while V-AUV is responsible for moving vertically between the surface and seabed to transmit the information. V-AUV improves energy efficiency by gathering information and uploads them to the surface station avoiding floating and diving movement of H-AUV.

Furthermore, the procedure of information exchange between H-AUVs and V-AUV can be model as a limited service vacation queueing system. With the construction and development of IoUT, peak AoI is of critical significance for supporting a range of time-sensitive applications, such as ocean environment monitoring and underwater salvage. In order to evaluate the timeliness of data sensed and utilized, we use peak AoI as a metric of the freshness of information, which is defined as the time elapsed since the generation time of the newest received packets update at a destination.

B. Underwater Acoustic Channel Analysis

Before deriving the peak AoI at the surface station, it is necessary to model the unique properties of underwater acoustic channel. We approximate the feature of the underwater acoustic channel for IoUT as [36] in order to obtain the channel capacity and derive the transmission energy consumption. Attenuation over a distance l and a signal of frequency f in an underwater acoustic channel is given by

$$A(l,f) = l^k a(f)^l \tag{1}$$

where k is the spreading factor, and $a(f)$ denotes the absorption coefficient. The acoustic path loss expressed in dB is expressed as

$$10 \log A(l,f) = k \cdot 10 \log l + l \cdot 10 \log a(f) \tag{2}$$

where the first term denotes the propagation loss, and the second term represents the absorption loss. The constant k ranges from 2 to 4. In general, let $k = 1.5$ represent the actual underwater acoustic propagation model. The absorption coefficient can be expressed in dB/km for f in kHz by using Thorp's empirical formula [37]

$$10 \log a(f) = \frac{0.11 f^2}{1+f^2} + \frac{44 f^2}{4100+f^2} + 2.75 \cdot 10^{-4} f^2 + 0.003. \tag{3}$$

The acoustic noise in an acoustic channel is the sum of four basic sources as follows:

$$N(f) = N_t(f) + N_s(f) + N_w(f) + N_{\text{th}}(f) \tag{4}$$

where $N_t(f), N_s(f), N_w(f)$, and $N_{\text{th}}(f)$ represent the most important underwater noisy sources, i.e., turbulence, shipping, waves, and thermal noise, respectively. Besides, the above power spectral density (p.s.d) of noise sources components in dB re μPa per Hz are obtained, i.e.,

$$10 \log N_t(f) = 17 - 30 \log f \tag{5a}$$

$$10 \log N_s(f) = 40 + 20\left(s - \frac{1}{2}\right) + 26 \log f - 60 \log(f + 0.03) \tag{5b}$$

$$10\log N_w(f) = 50 + 7.5w^{\frac{1}{2}} + 20\log f - 40\log(f + 0.4) \tag{5c}$$

$$10\log N_{\text{th}}(f) = -15 + 20\log f \tag{5d}$$

where s denotes the shipping activity ranging from 0 to 1, and w represents the wind speed with the unit m/s. The complex distance-bandwidth relationship is best explicated by the $1/AN$ factor over the different frequency and distance. Thus, the frequency-dependent part of narrow-band SNR with unit transmission power can be given by

$$\gamma(l, f) = \frac{1}{A(l, f)N(f)}. \tag{6}$$

Note that the underwater transmitter and receiver are narrow-band applications, thus the lower bound of the underwater acoustic channel capacity can be obtained using (6). Following the theoretical analysis in [38], it is worth noting that for a given transmission distance l, there exists an optimal frequency $f_{\max}$ for obtaining the maximum optimal SNR. In this section, let $\gamma(l, f_{\max})_{\max}$ be the optimal SNR with unit transmission power. We assume that the usable frequency range is $\mathcal{B} = [f_L(l), f_U(l)]$, where $\gamma(l, f_L(l)) = \gamma(l, f_U(l)) = \gamma(l, f_{\max}) -$ 3dB and the bandwidth is $B = f_U(l) - f_L(l)$. We assume the transmission distance l is less than 1 km, and the usable 3-dB frequency range $\mathcal{B}$ is dozens of KHz. Finally, we define the lower bounds function of SNR due to the harsh environment of the underwater acoustic channel, i.e.,

$$\widetilde{\gamma}(l) = \begin{cases} \min\left\{\gamma\left(l, f_c - \frac{B}{2}\right), \gamma\left(l, f_c + \frac{B}{2}\right)\right\}, & f \in \mathcal{B} \\ 0, & \text{Otherwise.} \end{cases} \tag{7}$$

For simplicity, $\widetilde{\gamma}(l)$ denotes the replacement of the real SNR function $\gamma(l, f)$. f_c is the center frequency. Without loss generality, based on additive white Gaussian noise (AWGN) channel, the channel capacity can be given by dividing into multiple narrow subbands as the sum of a single bandwidth. In the simplest case, we assume that the transmitted signal power spectral density (p.s.d.) $S(l, f)$ is flat within the bandwidth, $S(l, f) = P_{sl}/B$ for $f \in \mathcal{B}$, and 0 otherwise. Thus, the underwater acoustic channel capacity $C(l)$ can be obtained

$$\begin{aligned} C(l) &= \sum_{f \in \mathcal{B}} \Delta f \log_2\left(1 + \frac{S(l, f)A^{-1}(l, f_i)}{N(f_i)}\right) \\ &= B\log_2\left[1 + \frac{\eta P_{tr}\gamma(l_L, f)_{\min}}{2\pi \cdot (1\mu\text{Pa}) \cdot B}\right] \end{aligned} \tag{8}$$

where Δf denotes each frequency f_i, $(i = 1, 2, \ldots)$ subband-width, and let $A(l, f_i)$ and $N(f_i)$ be the corresponding constant attenuation factor and the p.s.d of noise; P_{tr} is the transmitted power in Watt; $1\mu\text{Pa} = 0.67 \times 10^{-18}$ W/m^2.

IV. Peak AoI Definition

Due to the underwater weak link between two IoUT nodes, AUVs are used as mobile relay to facilitate the underwater information collection. Considering the scenario we proposed, the IoUT nodes is divided into M clusters where a H-AUV are dispatched to collect data from K nodes in nth cluster. The set of nodes in nth cluster is denoted by $\mathcal{M}_n = \{\mathcal{M}_{n,1}, \ldots, \mathcal{M}_{n,k}, \ldots, \mathcal{M}_{n,k}\}$. Moreover, we assume that each

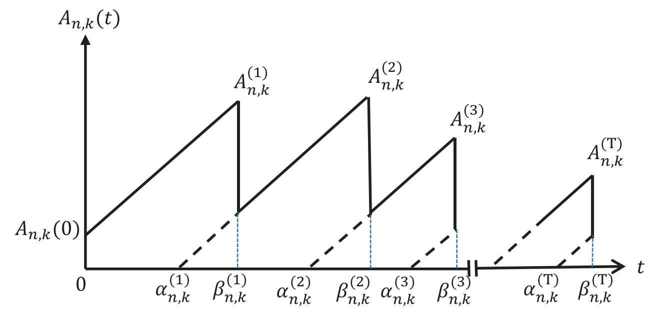

Fig. 2. AoI as a time function at the $\mathcal{M}_k$ IoUT node.

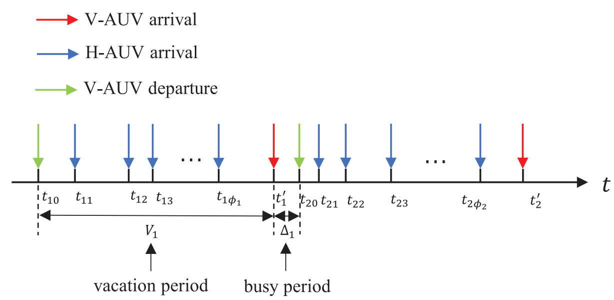

Fig. 3. Time instants of arrival and departure for the queueing system.

IoUT node updates the timestamped data with the fixed update rate. In order to collect the information, each H-AUV starts from the V-AUV seabed position υ^0 and moves to corresponding cluster to collect information following a prescheduled trajectory. After the procedure of collecting information from K nodes, the nth H-AUV returns back to the queueing system in υ_0 and wait for offloading the data on V-AUV. The time average waiting time W in queueing system is directly proportional to the peak AoI. In this section, we obtain the relationship between peak AoI, W and trajectory distance.

In most IoUT application scenarios, the timestamps are added to each packet by the senders, which can be used to obtain the AoI of IoUT system. Moreover, $g(t)$ represents the latest information generation time, and its corresponding information has been delivered at the destination. So the instantaneous AoI function can be given by

$$A(t) = t - g(t). \tag{9}$$

In Fig. 3, we use a graphical argument to show a sample variation of the AoI function $A_{n,k}(t)$ for $\mathcal{M}_{n,k}$ node. Without loss of generality, we assume that the IoUT nodes generate data with the Poisson parameters of packets arrival λ_n. Besides, in the jth cycle of information collection, IoUT node $\mathcal{M}_{n,k}$ updates its information through the corresponding H-AUV at $\alpha_{n,k}^{(j)}$. After the information exchange between H-AUVs and V-AUV in queueing system, data has been transmitted to surface station by V-AUV at $\beta_{n,k}^{(j)}$. Next, we derive the peak status update age function over time t for node $\mathcal{M}_{n,k}$ considering the statistical characteristics impact on AoI.

In our considering scenario, we only investigate the peak AoI at $\beta_{n,k}^{(j)}$ as the metric for evaluating the freshness of information collected by AUVs. Let $A_{n,k}^{(j)}$ denote the peak AoI value in the jth cycle, and W represents the waiting time in the queueing system. The definitions of T_U and T_D are given by (26); Moreover, L denotes the length of each packet, and $\mathbb{E}[N_{n,k}]$ is the expected number of packets collected in one cycle, i.e.,

$$\mathbb{E}[N_{n,k}] = \frac{C(h)\lambda_n\left[V_S\sum_{k=1}^{K} d_{n,k} + V_A V_S \mathbb{E}[W] + V_A K h\right]}{V_A V_S[C(h) - \lambda_n KL]} \tag{10}$$

where $d_{n,k}$ denotes the kth segment of the total H-AUV's trajectory. $C(h)$ represents the acoustic channel capacity in the condition of h, which is derived in (8). Apparently, the following inequality constraints should be satisfied to make the (10) true

$$C(h) > \lambda_n KL \tag{11}$$

which indicates the upper bound of the update rate of IoUT nodes with the fixed acoustic channel capacity $C(h)$. In order to obtain the expected value of peak AoI, i.e., $\mathbb{E}[A^P_{n,k}]$, we should first derive the expected time interval of $\Delta\boldsymbol{\beta}$ and $\Delta\boldsymbol{\alpha}$, where $\Delta\boldsymbol{\beta}$ is the expected time interval between two information updates by V-AUV in the surface station (destination), while $\Delta\boldsymbol{\alpha}$ denotes the time interval between packet generation time and the time in the destination. According to Fig. 3, $\Delta\boldsymbol{\beta}$ consists of the time consumed of total nodes in trajectory and queueing system; thus we have

$$\begin{aligned}\Delta\boldsymbol{\beta} &= \mathbb{E}\left[\beta^{(i+1)}_{n,k}\right] - \mathbb{E}\left[\beta^{(i)}_{n,k}\right]\\ &= T_U + T_D + \mathbb{E}[W] + \sum_{z=1}^{K}\left[\frac{d_{n,z}}{V_A} + \frac{\mathbb{E}\left[N^{(j)}_{n,z}\right]L}{C(h)}\right]\end{aligned} \tag{12}$$

where i denotes the amount of information collection cycles for IoUT nodes. Similarly, $\Delta\boldsymbol{\alpha}$ represents the sum of time consumed between the arrival instant of H-AUV in node $\mathcal{M}_{n,k}$ and the end of information exchange in queueing system as follows:

$$\begin{aligned}\Delta\boldsymbol{\alpha} &= \mathbb{E}\left[\beta^{(i)}_{n,k}\right] - \mathbb{E}\left[\alpha^{(i)}_{n,k}\right]\\ &= T_U + \mathbb{E}[W] + \sum_{z=k}^{K}\left[\frac{d_{n,z}}{V_A} + \frac{\mathbb{E}\left[N^{(j)}_{n,z}\right]L}{C(h)}\right].\end{aligned} \tag{13}$$

The expected peak AoI $\mathbb{E}[A^P_{n,k}] = \Delta\boldsymbol{\beta} + \Delta\boldsymbol{\alpha}$, which is difficult to obtain optimal value. For simplicity, we use $\Theta_{n,k}(\mathbf{d}_n)$ and $\Psi_{n,k}(W)$ to represent the function of H-AUV trajectory and expected waiting time $\mathbb{E}[W]$, respectively. We have: $\mathbf{d}_n = (d_{n,1}, \dots, d_{n,K})$ is the vector of the distance between each node of trajectory. $\widetilde{D} = \mathbf{d}_n\mathbf{1}$ is the total distance of trajectory in nth cluster, which can be solved in Section V. $D^* = \sum_{z=k}^{K} d_{n,z}$ denotes the trajectory between node $\mathcal{M}_{n,k}$ and V-AUV position υ_0. Then, the expected value of peak AoI $\mathbb{E}[A^P_{n,k}]$ in node $\mathcal{M}_{n,k}$ is decomposed into the sum of independent variables $\Theta_{n,k}(\mathbf{d}_n)$ and $\Psi_{n,k}(W)$

$$\mathbb{E}\left[A^P_{n,k}\right] = \Theta_{n,k}(\mathbf{d}_n) + \Psi_{n,k}(W) \tag{14}$$

subject to

$$\Theta_{n,k}(\mathbf{d}_n) = T_U + \frac{\varphi}{V_A}\widetilde{D} + \frac{D^*}{V_A} \tag{15}$$

and

$$\Psi_{n,k}(W) = (\varphi + 2)\mathbb{E}[W] + \frac{\varphi K h}{V_S} \tag{16}$$

where $\varphi = ([(2K - k + 1)L\lambda_n]/[C(h) - \lambda_n KL])$ is a constant, which is independent of $\mathbf{d}_n$ and $\mathbb{E}[W]$. Considering (14), the minimization of peak AoI problem can be partitioned into two subproblems that optimize the expected waiting time $\mathbb{E}[W]$ and trajectory distance $\widetilde{D}$, respectively. After deriving the simplified peak AoI definition in this section, we formulate the trajectory scheduling as a combinatorial optimization problem, then the derivation of the expected waiting time $\mathbb{E}[W]$ in the queueing system can be obtained (see Section VI).

V. Trajectory Planning and Energy Constraints

When H-AUVs and V-AUV have teamed up for underwater information collection, the total energy consumption is related to different phases of the AUVs. According to the description of multi-AUV underwater information collection scheme above, there are three modes for H-AUVs, i.e., patrol phase, data exchanging phase and queueing phase.

Patrol Phase: In this phase, H-AUV finishes the data exchange of the previous IoUT node and moves to the next IoUT node. We first consider the period of a H-AUV cruising in the nth cluster. Let the trajectory vector be $\mathbf{P_n} = [s^{(1)}_n, s^{(2)}_n, \dots, s^{(k)}_n, \dots, s^{(K)}_n]$, where $s^{(k)}_n$ represents the kth node position in the trajectory of cluster $\mathcal{M}_n$. According to [39], the minimal AoI trajectory problem is a shortest Hamiltonian path problem. In order to portray the connection of each node, we use the binary variable matrix $\mathbf{Y}_{\mathbf{n}(K+1)\times(K+1)}$ as path planning matrix. $Y_n(i,j)$ denotes the corresponding element, which can only equal to 1 (connected) or 0 (disconnected). Likewise, let $\mathbf{D}_n$ be the Euclidean distance matrix and $D_n(i,j)$ be its element. Therefore, the time consumption of H-AUV mobility in the ith segment of trajectory $\mathbf{P_n}$ can be formulated as

$$T^H_{P_{n,i}} = \frac{\mathbf{D}_n(\mathbf{Y_n}(i)\mathbf{V}_n, \mathbf{Y_n}(i+1)\mathbf{V}_n)}{V_A} \tag{17}$$

where the vector $\mathbf{V}_n = [1, 2, 3, \dots, K]^T$ and $\mathbf{Y_n}(i)$ denotes the ith row of matrix $\mathbf{Y_n}$. Thus, the total time consumption of H-AUV mobility in nth cluster can be obtained

$$T^H_{P_n} = \sum_{i=1}^{K+1} T^H_{P_{n,i}}. \tag{18}$$

Now it is clear that the total energy consumption of patrol phase in nth cluster is $E^H_{P_n} = P_A T^H_{P_n}$ under the energy constraint $E^H_{P_{n,\max}}$. Therefore, we can find the optimal $\widetilde{D}$ by the following mixed-integer programming problem, i.e.,

$$\min_{Y_{n,i,j}} \widetilde{D} = \sum_{j=1}^{K+1}\sum_{i=1, i\neq j}^{K+1} D_n(i,j)\cdot Y_n(i,j)$$

$$\text{s.t.} \sum_{j=1}^{K+1} Y_n(i,j) = 1,\ i = 1, 2 \dots, K+1 \tag{19a}$$

$$\sum_{i=1}^{K+1} Y_n(i,j) = 1,\ j = 1, 2 \dots, K+1 \tag{19b}$$

$$Y_n(i,j) \in \{0,1\},\ \ i,j = 1,2,\ldots,K+1 \tag{19c}$$

$$u_i - u_j + 1 \le K_n(1 - Y_n(i,j)),\ \ 2 \le i,j \le K+1 \tag{19d}$$

$$E^H_{P_n} \le E^H_{P_{n,\max}} \tag{19e}$$

where u_i is an auxiliary variable, which denotes the number of nodes visited when starting from the first node and arriving at ith node. In order to find the global optimal solution for relatively small scale IoUT nodes deployment scenarios, the Branch and Bound (B&B) algorithm can use to solve the above optimization problem [40]. However, B&B algorithm has a very high computational complexity. Therefore, inspiring by [12], we utilize genetic algorithm (GA) to find the near-optimal path for H-AUV information collection.

Data Exchanging Phase: H-AUV hovers over the seabed and collects information from IoUT nodes. Let L represent the packet length in nth cluster for each data update. Moreover, the sources generate updates, which is satisfied Poisson distribution with rate λ_n. Thus we get the expected value of L as follows:

$$\begin{aligned}\mathbb{E}[L_n] &= N\left(\widetilde{D} + W + \sum_{k=1}^{K}\Gamma_{n,k}\right)\cdot L\\ &= \lambda_n \cdot \left\{\mathbb{E}[\widetilde{D}] + \mathbb{E}[W] + \sum_{k=1}^{K}\mathbb{E}[\Gamma_{n,k}]\right\}\cdot L\end{aligned} \tag{20}$$

where $N(t)$ denotes the number of H-AUVs arriving within time t; $\Gamma_{n,k}$ is the transmission time consumed in node $\mathcal{M}_{n,k}$. When the system reaches a steady-state distribution, we assume that the expected data length of each IoUT node updated during $\widetilde{D} + W$ should be the same. Moreover, the expected data transmission time $\Gamma_{n,k}$ for kth IoUT node in nth cluster can be obtained

$$\mathbb{E}[\Gamma_{n,k}] = \frac{h}{V_S} + \frac{\mathbb{E}[L]}{C(h)} \tag{21}$$

where V_S denotes the speed of sound underwater. Therefore, the nth cluster total time consumption of information collection is $\Gamma_n = \sum_{k=1}^{K}\Gamma_{n,k}$. Moreover, under the assumption of steady distribution, we have the expected value of total transmission time $\mathbb{E}[\Gamma_n] = K\cdot\mathbb{E}[\Gamma]$ if each node has the same expected update rate $\mathbb{E}[\Gamma]$. By considering the (20) and (22), we get the final expression for the expected data transmission time as follows:

$$\mathbb{E}[\Gamma_n] = \frac{KhC(h) + K\lambda_n L V_S\left\{\mathbb{E}[\widetilde{D}] + \mathbb{E}[W]\right\}}{V_S\{C(h) - \lambda_n L K\}}. \tag{22}$$

Let P_w and P_{re} be the H-AUV hovering power and the transmission power respectively. Therefore, the data exchanging phase energy consumption of H-AUV in nth cluster can be given by

$$E^H_{T_n} = (P_w + P_{re})\cdot\mathbb{E}[\Gamma_n]. \tag{23}$$

Moreover, the K nodes total energy consumption of data exchanging phase in the cluster $\mathcal{M}_n$ can be obtained as follows:

$$E^S_{T_n} = P_{tr}\cdot\mathbb{E}[\Gamma_n]. \tag{24}$$

Queueing Phase: This phase falls into two categories. First, the vacation period contains the floating and diving time of V-AUV, during which V-AUV can not provide information exchange service to H-AUVs in the queueing system. Second, the busy period that consists of the time of exchange information between H-AUVs and V-AUV with FCFS service discipline. The total expected energy consumption E^H_w for one H-AUV in queueing phase is

$$E^H_w = P_w\mathbb{E}[W] \tag{25}$$

where $\mathbb{E}[W]$ denotes the expected value of waiting time W. Moreover, we assume that the H-AUVs are able to exchange information with V-AUV in a high transmission rate for the short distance of communication. Thus, the service time and energy consumption during busy period can be ignored comparing to the AUV movement time consumed. After the busy period, V-AUV, as an information mobile "relay", have to leave queueing system in υ_0 to update information in surface station. V-AUV round trip energy consumption can be expressed as

$$E^V_r = P_U\cdot\frac{H_R}{V_U} + P_D\cdot\frac{H_R}{V_D} = P_U\cdot T_U + P_D\cdot T_D \tag{26}$$

where P_U and P_D are the floating and diving power of V-AUV in the vertical depth of H_R, respectively; V_U and V_D are the velocity of the floating and diving, respectively.

VI. Limited Service Queueing Model

A. Derivation of Steady Distribution

After collecting the data from IoUT nodes, the H-AUVs of each cluster move to the position of V-AUV and wait to exchange the data collected from IoUT nodes. In this heterogeneous information collection system, we assume that the V-AUV has ability to collect data with H-AUVs during the busy period. To further simplify the model, all H-AUVs' arrivals at queueing system subject to Poisson process with parameter $\widetilde{\lambda}$. Let L^*_i be the number of H-AUVs waiting in the queueing system while V-AUV comes back from the surface station. Considering the constraint of V-AUV storage and energy consumption, we define M as the upper limit for the number of AUVs served during the busy period.

Fig. 3 depicts the procedure of H-AUVs' arrival and the information exchange in queueing system. Let V_i and Δ_i be the ith vacation period and V-AUV information collection time, i.e., the busy period, respectively. Besides, $t_{i1}, t_{i2}, \ldots, t_{i\Phi_i}$ denote the time of H-AUVs arrival, which indicates the number of H-AUVs served would not exceed the Φ_i during ith busy period. In the proposed queueing system, the number of customers served in ith busy period should be

$$\Phi_i = \min\left(L^*_i, M\right) \tag{27}$$

where indicates the number of H-AUVs served by V-AUV during one busy period is not more than M and H-AUVs arrived during the busy period have to wait for the next busy period. According to the definition of L^*, we get the fact that $\{L^*_i, i \ge 1\}$ is a homogeneous Markov chain. Let $V(t)$ be the stochastic variable distribution function of the vacation period. Similarly, let $B_i(t)$ be the distribution function of information exchange time for ith H-AUV. Besides, let $\Omega_j = V + \sum_{t=1}^{j} B_t$ denote the total service period of all AUVs in the queue plus one vacation period. Thus we obtain

$$L_{i+1}^* = \left(L_i^* - M\right) \cdot \epsilon\left(L_i^* - M\right) + N\left(V + \sum_{t=1}^{\Phi_i} B_t\right) \quad (28)$$

where the first term represents the number of H-AUV finished information exchange within ith busy period, and the second term denotes the H-AUVs' arrivals within ith busy period and vacation period. Besides, the definition of $\epsilon(x)$ is

$$\epsilon(x) = \begin{cases} 1, & x > 0 \\ 0, & x \le 0. \end{cases} \quad (29)$$

According to (28), $\{L_i^*, i \ge 1\}$ is an embedded Markov chain of the queueing process. Thus, we can get the transition probability of this Markov chain P_{jk} according to Lemma 1. The steady-state distribution of the Markov chain can be given by

$$\begin{aligned} q_k &= \lim_{i\to\infty} P_r\left\{L_i^* = k\right\} \\ &= \lim_{i\to\infty} \sum_{j=0}^{\infty} P_r\left\{L_i^* = k | L_{i-1}^* = j\right\} P_r\left\{L_{i-1}^* = j\right\} \\ &= \sum_{j=0}^{M-1} \int_0^{\infty} \frac{\left(\widetilde{\lambda} t\right)^k}{k!} e^{-\widetilde{\lambda} t} dP_r\{\Omega_j < t\} q_j \\ &\quad + \sum_{j=M}^{k+M} \int_0^{\infty} e^{-\widetilde{\lambda} t} \frac{\left(\widetilde{\lambda} t\right)^{k-j+M}}{(k-j+M)!} dP_r\{\Omega_M < t\} q_j, \ k \in \mathbb{N} \end{aligned} \quad (30)$$

where $Q(z)$ denotes the probability-generating function (p.g.f.) of $\{q_k, k \ge 0\}$, which can be derived by Lemma 2. We assume that V-AUV's floating and diving speed remains constant, namely V_U and V_D, respectively. Therefore, the amount of time elapsed during vacation period in the queueing system can be considered a constant as follows:

$$T_{UD} = H_R\left(\frac{1}{V_U} + \frac{1}{V_D}\right) \quad (31)$$

where H_R denotes the depth of υ_0. Because the exchange information time much shorter than AUV movement time, the time consumed during busy period can be ignored. Thus, the probability density function (p.d.f.) of time consumed during vacation period and busy period of V-AUV are $v(t) = \delta(t - T_{UD})$ and $b(t) = \delta(t)$ respectively. $\delta(t)$ is Dirac delta function. Therefore the Laplace Transform (L.T.) of the vacation time and the service time can be given by $V^*(s) = e^{-T_{UD}s}$ and $B^*(s) = 1$. So, the p.g.f. of the number of H-AUVs waiting in the queueing system $Q(z)$ can be derived as

$$Q(z) = \frac{e^{-T_{UD}s}\left\{z^M Q_M(1)\right\} - Q_M(z)}{z^M - e^{-T_{UD}s}} \quad (32)$$

where $Q_M(z) = \sum_{j=0}^{M-1} q_j z^j$. Relying on Lemma 3, we assume the steady-state condition $\widetilde{\lambda} T_{UD} < M$ is hold and the expected value of the number of queueing H-AUVs while the finish of the vacation period $\mathbb{E}[L^*]$ is given by

$$\begin{aligned} \mathbb{E}\left[L^*\right] &= \left.\frac{dQ(z)}{dz}\right|_{z=1} \\ &= \frac{1}{2(M - \widetilde{\lambda} T_{UD})} \\ &\quad \times \left\{\left(\widetilde{\lambda} T_{UD}\right)^2 + 2\widetilde{\lambda} T_{UD}\left(M - \widetilde{\lambda} T_{UD}\right)\right. \\ &\quad \left. - \left[Q_M^{(2)}(1) + M(M-1)(1 - Q_M(1))\right]\right\}. \end{aligned} \quad (33)$$

According to Lagrange's theorem and Rouché's theorem [41], we can therefore derive the coefficient of $Q(z)$ by addressing the issue of the following linear equations, i.e.,

$$\begin{cases} \sum_{k=0}^{M-1} q_k\left\{Z_m^M - Z_m^k\right\} = 0 \\ \sum_{k=0}^{M-1} (M-k) q_k = M - \widetilde{\lambda} T_{UD} \\ Z_m = \sum_{n=1}^{\infty} \frac{e^{j\frac{2\pi mn}{M}}}{n!} \cdot \frac{d^{n-1}}{dZ^{n-1}} \left[e^{-\widetilde{\lambda}(1-z)T_{UD}}\right]^{\frac{n}{M}}\Bigg|_{z=0} \end{cases} \quad (34)$$

where $m = 1, 2, \ldots, M-1$ and $j = \sqrt{-1}$ denotes imaginary number. Using the stochastic decomposition theorem, the waiting time variable of H-AUVs in queueing system W can be decomposed into three independent random variables as follows:

$$W = W_{M/G/1} + W_d + W_r \quad (35)$$

where $W_{M/G/1}$ denotes the waiting time of a general M/G/1 queue without vacation. Besides, W_d and W_r are the additional latency owing to the vacation period T_{UD} influence. For the sum of independent statistical variables W, the corresponding p.g.f. has a product-form function, and thus the L.T. of W can be given by

$$\begin{aligned} W^*(s) &= W_{M/G/1}^*(s) \cdot W_d{}^*(s) \cdot W_r{}^*(s) \\ &= \frac{1}{s} \cdot \frac{1 - e^{-T_{UD}s}}{T_{UD}} \cdot \frac{Q\left(1 - s/\widetilde{\lambda}\right)}{e^{-T_{UD}s}}. \end{aligned} \quad (36)$$

From this expression, we can derive the expected value of H-AUVs waiting time $\mathbb{E}[W]$ by the following equation:

$$\begin{aligned} \mathbb{E}[W] &= -\left.\frac{dW^*(s)}{ds}\right|_{s=0} \\ &= \frac{\mathbb{E}\left[L^*\right]}{\widetilde{\lambda}} - \frac{T_{UD}}{2}. \end{aligned} \quad (37)$$

Substituting $\widetilde{D}$, (37) and (33) into (14), we can obtained a expected peak AoI function of the upper bound M.

B. AoI-Inspired Problem Formulation

The energy constraints of the system include the resources consumption of H-AUV, sensor transmission and V-AUV. To evaluate the energy efficiency of the system, we define the total sum of energy consumption function as

$$\mathcal{E}\left(M, \widetilde{\lambda}, \lambda_n\right) = E_n^H + \frac{E_r^V}{\mathbb{E}[\Phi]} + E_{T_n}^S \quad (38)$$

where $E_n^H = E_{P_n}^H + E_{T_n}^H + E_w^H$ is the energy consumption of H-AUV. For the purpose of optimizing the peak AoI of system proposed, we formulate the optimization problem subject to energy consumption constraints as follows:

$$\begin{aligned} \min_{M} \ & \mathbb{E}\left[A_{n,k}^P\right] \\ \text{s.t.} \ & 0 \le \mathcal{E}\left(M, \widetilde{\lambda}, \lambda_n\right) \le \mathcal{E}_{\max} \end{aligned} \quad (39a)$$

$$M_{\min} \le M \le M_{\max} \tag{39b}$$
$$0 \le E_n^H \le E_{n\ \max}^H \tag{39c}$$
$$0 \le E_{T_n}^S \le E_{T_n \max}^S \tag{39d}$$

where (39a) is the constraints of energy consumption and peak AoI, respectively; (39b) denotes the maximum upper for the number of H-AUVs served. Besides, $M_{\min} = \widetilde{\lambda} T_{UD} + \epsilon$ and $\epsilon \in (0, 1)$, which are derived from the steady-state condition of queueing system. According to (14), peak AoI is divided into the sum of functions of two independent variable, i.e., $\widetilde{D}$ and $\mathbb{E}[W]$. The near-optimal trajectory of H-AUV $\widetilde{D}$ is solved in Section V. In order to minimize $\mathbb{E}[W]$, we design an adaptive algorithm for adjusting the upper bound of length in queueing system in Algorithm 1 based on steady condition and the search of the optimal M. Through the major procedures of the algorithm, we obtain the stationary distribution of system states and the near-optimal limited upper bound value M with low-complexity to minimize $\mathbb{E}[W]$.

C. Computational Complexity Analysis

In terms of the computational complexity, Algorithm 1 considers $i_{\max}$ iterations of the update of the upper band of the queue length M. When algorithm calculates $Q(z)$, its upper bound of the iteration is infinite, which is far beyond the range of possibility to obtain practical value. In order to reduce the computational complexity, let N^* be a constant to replace the upper bound of summation, because $1/n!$ is too small to make a difference comparing to the value of Z_m. Therefore, during the each iteration, the computational complexity of calculating the target value M coefficients in (32) is $O(N^*(M-1)^2)$. Considering the iteration times of the outermost loop, the worst computational complexity of Algorithm 1 should be $O(i_{\max} N^*(M-1)^2)$.

VII. Simulation Results and Discussion

Simulations are carried out to demonstrate the outperformance of multi-AUV-assisted heterogeneous underwater information collection scheme we proposed by using MATLAB. First, we introduce the scenario setup for simulations. We assume that one H-AUV solves the mixed-integer programming problem and gets the near optimal trajectory in advance. Then, H-AUV follows the trajectory and collects the information from IoUT nodes. After H-AUV finishes the information collection, it moves to the V-AUV position υ_0 and exchanges data with V-AUV during the busy period.

Fig. 4 shows the coordinates of nodes and the trajectory scheduling result. Therefore, the trajectory vector can be set as $\mathbf{P_n} = [(310, 110), (242, 121), \ldots, (80, 282), \ldots, (282, 162)]$. We assume the middle node position is (80, 828), where $K = 19$, $k = 10$. Besides, the acoustic transmission frequency is 25 kHz with bandwidth $\varpi = 1$ kHz. The upper bound of energy constraints (39a) is $\mathcal{E}_{\max} = 1.8 \times 10^6$ J. The maximum queue length $M_{\max} = 10$ and the minimum value $M_{\min} = \widetilde{\lambda} T_{UD}$ for the queueing stability. Single AUV scheme means that the information collection for IoUT nodes is carried out by one AUV. In order to reduce peak AoI in single AUV scheme, AUV is capable of adjusting 2-D movement speed under the constraint of energy cost (less than $1.6\mathcal{E}$). Other detailed parameters are summarized in Table I.

Algorithm 1: Adaptively Adjusting Method for the Upper Limit of the Queuing Length M

Data: $\widetilde{\lambda}$, λ_n, T_{UD};
Result: $\mathbb{E}[W^\star]$, $\mathbb{E}[L^\star]$, $M^\star$;
Initialize peak AoI $\mathbb{E}[A_{n,k}^P]^{(0)} \leftarrow 0$, $i \leftarrow 0$;
Initialize the upper limit $M^{(0)} \leftarrow \lceil \widetilde{\lambda} \cdot T_{UD} \rceil$;
Set the maximum number of iteration indicator i_{max};
while $M^{(i)} \le M_{max}$ and $i \le i_{max}$ **do**
  Calculate the coefficient: Z_m, $m = 1, 2, \ldots, M^{(i)} - 1$;
  Substituting $Z = [Z_1, Z_2, \ldots, Z_{M-1}]$ in (34);
  Getting a polynomial $Q_M(z)$;
  Obtain $\mathbb{E}[W]$ and $\mathbb{E}[L]$ by (33) and (37);
  if $\mathbb{E}[W^\star]^{(i)} < \mathbb{E}[W^\star]^{(i-1)}$ **then**
    $M^\star \leftarrow M^{(i)} + n$, $\mathbb{E}[W^\star] \leftarrow \mathbb{E}[W]$;
    $\mathbb{E}[L^\star] \leftarrow \mathbb{E}[L]$;
  end
  $i \leftarrow i + 1$;
end

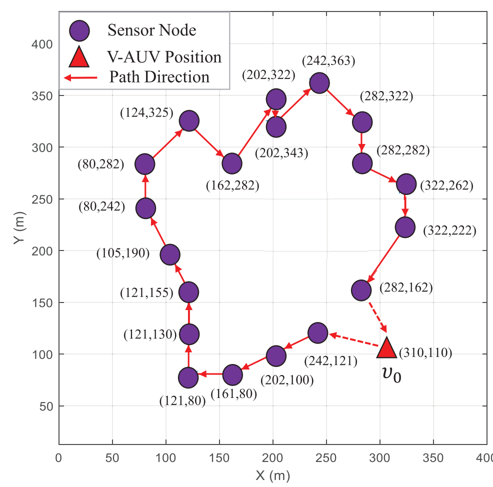

Fig. 4. Near-optimal path with sensor nodes $K_n = 19$ in the nth cluster.

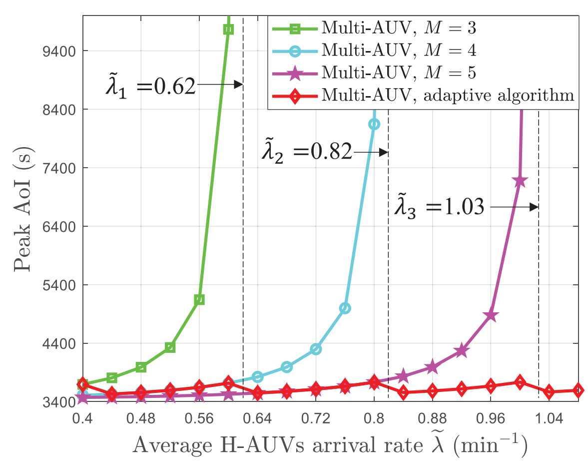

Fig. 5. Peak AoI with different arrival rate of H-AUVs.

Fig. 5 depicts the peak AoI under different arrival rate of H-AUVs $\widetilde{\lambda}$ with respect to $\lambda_n = 0.6$ s^{-1} and $h = 10$ m. The length of packet L is 1024 b. It can be observed that

TABLE I
SIMULATION PARAMETERS

Parameters	Values
Number of nodes in n-th clusters (K)	19
Underwater sound propagation speed (V_S)	1500 m/s
Transmission power (P_{tr})	30 mW
Receiving power (P_{re})	10 mW
Acoustic signal frequency (f_{tr})	25 kHz
Circuit efficiency (η)	20 %
Update packet length (L)	1024 bit
Spreading factor (k)	1.5
Shipping activity factor(s)	0.5
Wind speed (w)	0 m/s
H-AUV's hovering height (h)	10 m
H-AUV's velocity (V_A)	5 knot
H-AUV's flying power (P_f)	2 kW
H-AUV's waiting/hovering power (P_w)	0.2 kW
V-AUV's diving power (P_D)	5 kW
V-AUV's floating power (P_U)	6 kW
H-AUV's floating velocity (V_U)	1 knot
H-AUV's diving velocity (V_D)	2 knot

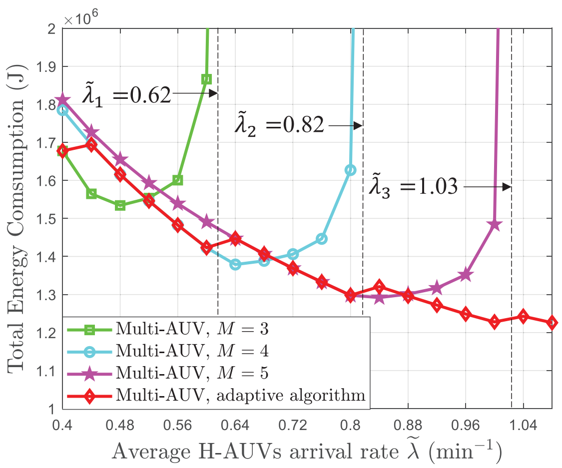

Fig. 6. Average energy consumption of total system under different arrival rate of H-AUVs.

our proposed heterogeneous scheme with adaptive algorithm outperforms the multi-AUV schemes without the adaptive algorithm in terms of peak AoI. It's because the proposed algorithm can find near-optimal upper bound of queue length M to keep the queueing system stable. With the arrival rate of H-AUV $\widetilde{\lambda}$ increases, the queuing systems are overloaded without adaptive algorithm ($M = 3$, $M = 4$, $M = 5$), which lead to the augment of peak AoI and queue instability, while using the adaptive algorithm makes queue stable and minimize peak AoI.

Fig. 6 illustrates the energy efficiency of the AUVs. With the growth of the number of H-AUVs served in busy period, average energy consumption for a period of information collection tends to decrease, which improves the energy efficiency of IoUT. However, the multi-AUV schemes tend to become unstable if the stable condition is not met. It can be seen that our proposed adaptive algorithm can improve the energy efficiency of the multi-AUV information collection system.

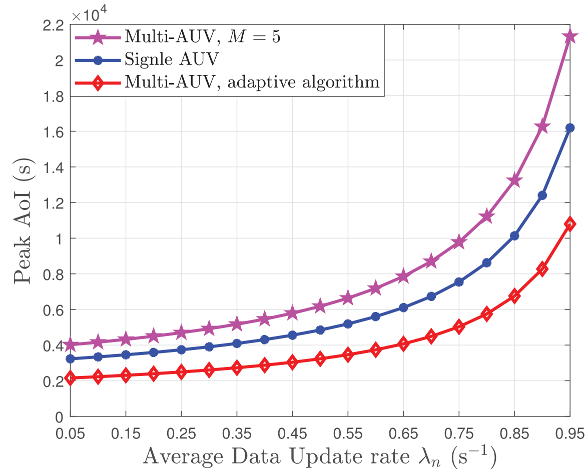

Fig. 7. Peak AoI with the different update data rate.

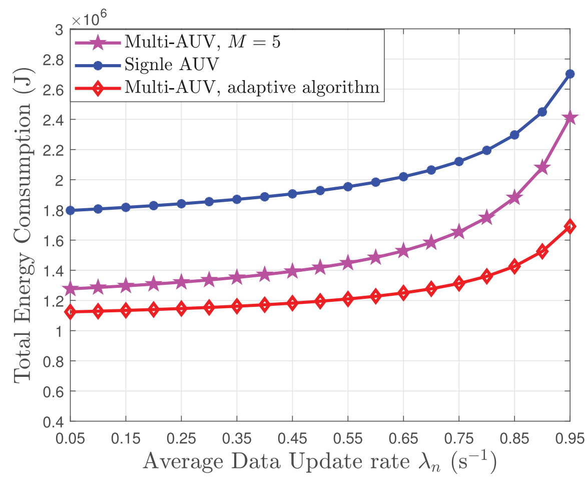

Fig. 8. Average energy consumption of total system with the different update data rate.

Fig. 7 shows the impact of the average nodes data update rate λ_n on the peak AoI by comparing the multi-AUV schemes and the single AUV scheme. The average H-AUV arrival rate is $\widetilde{\lambda} = 1$ min^{-1} and the hovering distance of H-AUV is $h = 10$ m. The length of packet is 1024 b. With the growth of λ_n, the peak AoI increases because the information collection consumes more time. It can be seen that our proposed algorithm has a lower peak AoI comparing with another schemes. Fig. 8 demonstrates the performance of energy efficiency versus different average data update rate in different schemes. It can be observed that the energy consumption of each scheme increases with the augment of λ_n. Moreover, our proposed scheme with adaptive algorithm always outperforms the comparison schemes in terms of all given λ_n. It is because that our proposed algorithm considers the stability of queueing system and adjusts the upper limit of the queuing length M for the sake of reducing the average energy consumption.

The sensor nodes update the binary large object data, such as video, audio or image. Media resources lead to the augment of packet length L. Next we focus on the schemes performance of peak AoI and energy efficiency with different length of packet L in Figs. 9 and 10, respectively. We assume $\widetilde{\lambda} =$

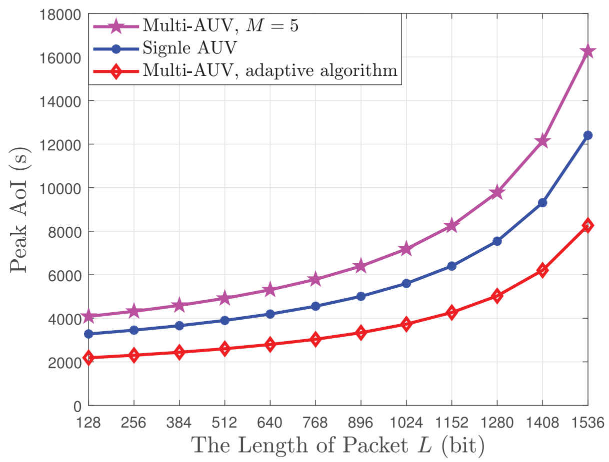

Fig. 9. Peak AoI with the different length of packet updated L.

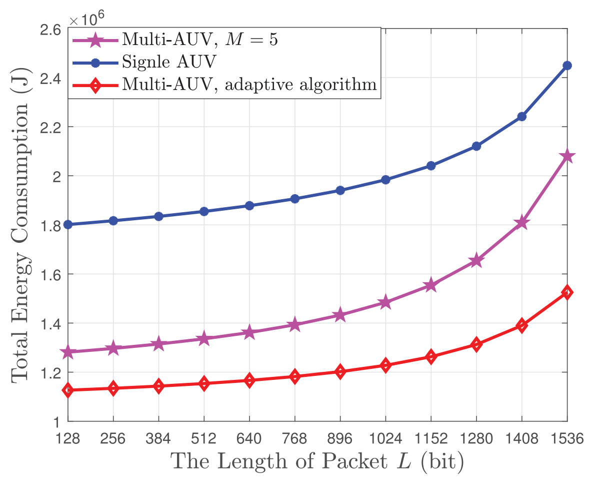

Fig. 10. Average energy consumption of total system with the different length of packet updated L, and the H-AUV arrival rate is set as $\widetilde{\lambda} = 1$ min^{-1}.

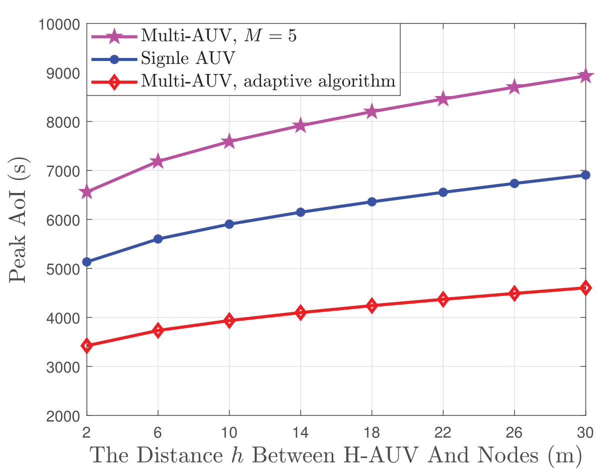

Fig. 11. Peak AoI with the different depth of H-AUV.

1 min^{-1}, $\lambda_n = 0.6$ s^{-1} and $h = 10$ m. With the growth of L, the workload of H-AUV transmission and the time consumed increase with the high energy consumption. It can be seen that our proposed scheme with adaptive algorithm has a lower peak AoI and energy consumption when the length of packet increases. It is because that the adaptive algorithm is more suited to the large size workload by adjusting the queueing length.

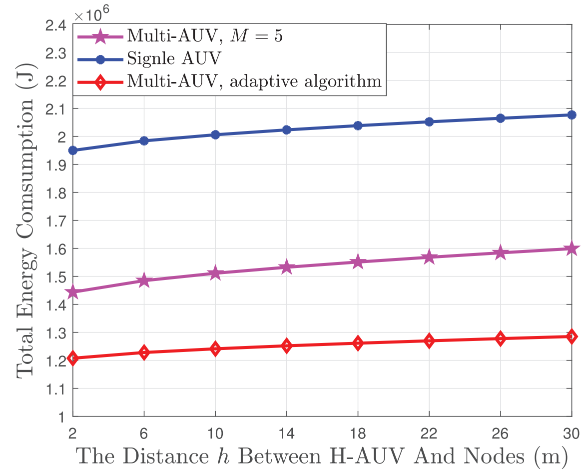

Fig. 12. Average energy consumption of total system with the different depth of H-AUV.

Figs. 11 and 12 portray the trend of peak AoI and energy efficiency with H-AUV different depth h, respectively. We set $\widetilde{\lambda} = 1$ min^{-1}, $\lambda_n = 0.6$ s^{-1} and $L = 1024$ b. Since the complex terrain of the seabed affects the hover height of H-AUV for the safety of movement, which changes transmission channel capacity according to (8). It can be seen that the energy consumption and peak AoI are increasing with the growth of h. The acoustic attenuation coefficient increases with the growth of h causing the signal rate degradation, which makes the system energy efficient with high AoI. As shown in the our proposed algorithm has a better peak AoI and energy-efficiency performance at all h.

VIII. Conclusion

In this article, we studied a multi-AUV-assisted heterogeneous underwater information collection scheme for IoUT. After analyzing the underwater acoustic channel and trajectory planning problem, we used the limited service M/G/1 vacation queueing system to model the process of information exchange and derived the steady-state distribution of the queue length. Then, a low-computational algorithm is proposed for adaptively adjusting the upper limit of the queuing length in order to minimize peak AoI under the energy constraint. Finally, the extensive simulations were conducted and results validates that our proposed AUV-assisted information collection scheme makes a better tradeoff between AoI and energy consumption than other schemes.

Appendix A
Theorem and Lemma

Lemma 1: For all limited service M/G/1 queues that satisfy (27), the one-step transition probability p_{jk} can be given by

$$p_{jk} = \begin{cases} \int_0^\infty e^{-\widetilde{\lambda}t} \frac{(\widetilde{\lambda}t)^{k-j+M}}{(k-j+M)!} dP_r\{\Omega_M < t\}, & k \geq j - M \geq 0 \\ \int_0^\infty e^{-\widetilde{\lambda}t} \frac{(\widetilde{\lambda}t)^{k}}{k!} dP_r\{\Omega_j < t\}, & j < M \\ 0, & \text{otherwise.} \end{cases} \quad (40)$$

Proof: According to the balance equation ((28)) and the upper limit function (27), the one-step transition probability p_{jk} for the limited service queueing system needs to discuss separately with different j and k.

First, after the V-AUV comes back from its "vacation" period, H-AUVs in the queue L_j^* are not less than M (the upper length limit of the queueing system). Then the next time V-AUV finishes vacation, the number of AUVs must be no less than $L_j^* - M$, thus we obtain

$$\begin{aligned} p_{jk} &= P_r\left\{L_{i+1}^* = k | L_i^* = j\right\} \\ &= P_r\{j - M + N(D_M) = k\},\ k \geq j - M \geq 0. \end{aligned} \quad (41)$$

When H-AUVs in the queue L_j^* are less than M, V-AUV exchange data with only L_j^* H-AUVs, and hence

$$p_{jk} = P_r\{N(\Omega_j) = k\},\ j < M. \quad (42)$$

Because other situations are impossible practically, we have $p_{jk} = 0$ when $j \geq M$ or $k < j - M$. ■

Lemma 2: The steady distribution p.g.f of the number of queueing AUVs after V-AUV exchanges data with surface station can be given by

$$\begin{aligned} Q(z) &= \sum_{j=0}^{M-1} q_j \left\{B^*\left[\widetilde{\lambda}(1-z)\right]\right\}^j V^*\left[\widetilde{\lambda}(1-z)\right] \\ &\quad + \sum_{j=M}^{\infty} q_j z^{j-M}\left[B^*\widetilde{\lambda}(1-z)\right]^M V^*\left[\widetilde{\lambda}(1-z)\right]. \end{aligned} \quad (43)$$

Proof: Substituting (30) in the definition of p.g.f $Q(z) = \sum_{k=0}^{\infty} q_k z^k$, we have

$$\begin{aligned} Q(z) &= \sum_{k=0}^{\infty} z^k \sum_{j=0}^{M-1} \int_0^{\infty} \frac{(\widetilde{\lambda}t)^k}{k!} e^{-\widetilde{\lambda}t} dP_r\{\Omega_j < t\} q_j \\ &\quad + \sum_{j=M}^{k+M} z^k \int_0^{\infty} e^{-\widetilde{\lambda}t} \frac{(\widetilde{\lambda}t)^{k-j+M}}{(k-j+M)!} dP_r\{\Omega_M < t\} q_j \\ &= \sum_{j=0}^{M-1} q_j \left\{B^*[\widetilde{\lambda}(1-z)]\right\}^j V^*[\widetilde{\lambda}(1-z)] \\ &\quad + \sum_{j=M}^{\infty} q_j z^{j-M}\left[B^*\widetilde{\lambda}(1-z)\right]^M V^*[\widetilde{\lambda}(1-z)] \end{aligned} \quad (44)$$

where B and $B^*(s)$ denote the service time of V-AUV and the corresponding L.T. function respectively. Similarly, V and $V^*(s)$ denote the vacation time of V-AUV and its L.T. function respectively. ■

Lemma 3: For the service time and vacation time of V-AUV are trending to zero and a constant respectively, the steady-state conditions of the limited service M/G/1 vacation queueing system can be obtained by

$$\widetilde{\lambda} T_{UD} < M. \quad (45)$$

Proof: The service time of V-AUV can be expressed as

$$T_S = \sum_{t=1}^{\Phi} B_t. \quad (46)$$

Thus we get the L.T. of the service time T_S

$$\begin{aligned} T_S{}^*(s) &= \sum_{k=0}^{\infty} \mathbb{E}\left[e^{s\sum_{t=1}^{\Phi} B_t}\right] P\{\Phi = k\} \\ &= \sum_{k=0}^{M-1} q_k \left[B^*(s)\right]^k + \sum_{k=M}^{\infty} q_k \left[B^*(s)\right]^M \\ &= Q_M\left[B^*(s)\right] + \left[B^*(s)\right]^M. \end{aligned} \quad (47)$$

Substituting the (32) and (34) in this expression, we can derive the expected value of the service time $\mathbb{E}[T_S]$ as follows:

$$\mathbb{E}[T_S] = \mathbb{E}[B]\left\{Q_M'(1) + M[1 - Q_M(1)]\right\} = \frac{\rho\mathbb{E}[V]}{1-\rho}. \quad (48)$$

The average number of H-AUVs served by V-AUV within one busy period must be less than M. Besides, with the service time B approach zero, the load on the above queue be given by $\rho = [(\widetilde{\lambda})/(\mathbb{E}[B]^{-1})] \to 0$. Then we get $\mathbb{E}[N(T_S + V)] = \widetilde{\lambda}\mathbb{E}[T_S + V] = \widetilde{\lambda}\mathbb{E}[V] < M$, where V is a constant T_{UD}. Thus the steady-state conditions of the limited service M/G/1 vacation queueing system $\widetilde{\lambda} T_{UD} < M$ can be proved. ■

REFERENCES

[1] F. Yin, G. F. John, J. S. Hayworth, and T. P. Clement, "Long-term monitoring data to describe the fate of polycyclic aromatic hydrocarbons in deepwater horizon oil submerged off alabama's beaches," *Sci. Total Environ.*, vol. 508, pp. 46–56, Mar. 2015.

[2] F. Thompson and D. Guihen, "Review of mission planning for autonomous marine vehicle fleets," *J. Field Robot.*, vol. 36, no. 2, pp. 333–354, Sep. 2019.

[3] Y. Wu, "Coordinated path planning for an unmanned aerial-aquatic vehicle (UAAV) and an autonomous underwater vehicle (AUV) in an underwater target strike mission," *Ocean Eng.*, vol. 182, pp. 162–173, Jun. 2019.

[4] T. Qiu, Z. Zhao, T. Zhang, C. Chen, and C. L. P. Chen, "Underwater Internet of Things in smart ocean: System architecture and open issues," *IEEE Trans. Ind. Informat.*, vol. 16, no. 7, pp. 4297–4307, Oct. 2019.

[5] S. Kaul, R. Yates, and M. Gruteser, "Real-time status: How often should one update?" in *Proc. IEEE Conf. Comput. Commun. (INFOCOM)*, Orlando, FL, USA, Mar. 2012, pp. 2731–2735.

[6] Y. Sun, E. Uysal-Biyikoglu, R. D. Yates, C. E. Koksal, and N. B. Shroff, "Update or wait: How to keep your data fresh," *IEEE Trans. Inf. Theory*, vol. 63, no. 11, pp. 7492–7508, Nov. 2017.

[7] R. Talak, S. Karaman, and E. Modiano, "Optimizing information freshness in wireless networks under general interference constraints," *IEEE/ACM Trans. Netw.*, vol. 28, no. 1, pp. 15–28, Feb. 2019.

[8] F. A. de Souza, B. S. Chang, G. Brante, R. D. Souza, M. E. Pellenz, and F. Rosas, "Optimizing the number of hops and retransmissions for energy efficient multi-hop underwater acoustic communications," *IEEE Sensors J.*, vol. 16, no. 10, pp. 3927–3938, May 2016.

[9] P. Gjanci, C. Petrioli, S. Basagni, C. A. Phillips, L. Boloni, and D. Turgut, "Path finding for maximum value of information in multi-modal underwater wireless sensor networks," *IEEE Trans. Mobile Comput.*, vol. 17, no. 2, pp. 404–418, Feb. 2018.

[10] N. Li, J.-F. Martínez, J. M. M. Chaus, and M. Eckert, "A survey on underwater acoustic sensor network routing protocols," *Sensors*, vol. 16, no. 3, p. 414, Mar. 2016.

[11] R. Su, D. Zhang, C. Li, Z. Gong, R. Venkatesan, and F. Jiang, "Localization and data collection in AUV-aided underwater sensor networks: Challenges and opportunities," *IEEE Netw.*, vol. 33, no. 6, pp. 86–93, May 2019.

[12] R. Duan, J. Du, C. Jiang, and Y. Ren, "Value based hierarchical information collection for AUV enabled Internet of Underwater Things," *IEEE Internet Things J.*, vol. 7, no. 10, pp. 9870–9883, May 2020.

[13] K. Zhang, J. Du, J. Wang, C. Jiang, Y. Ren, and A. Benslimane, "Distributed hierarchical information acquisition systems based on AUV enabled sensor networks," in *Proc. IEEE Int. Conf. Commun. (ICC)*, Shanghai, China, May 2019, pp. 1–6.

[14] J. Yan, X. Yang, X. Luo, and C. Chen, "Energy-efficient data collection over AUV-assisted underwater acoustic sensor network," *IEEE Syst. J.*, vol. 12, no. 4, pp. 3519–3530, Dec. 2018.

[15] G. Han, X. Long, C. Zhu, M. Guizani, and W. Zhang, "A high-availability data collection scheme based on multi-AUVs for underwater sensor networks," *IEEE Trans. Mobile Comput.*, vol. 19, no. 5, pp. 1010–1022, Mar. 2019.

[16] C. Wang, L. Wei, Z. Wang, M. Song, and N. Mahmoudian, "Reinforcement learning-based multi-AUV adaptive trajectory planning for under-ice field estimation," *Sensors*, vol. 18, no. 11, pp. 38–59, Oct. 2018.

[17] M. A. Abd-Elmagid, N. Pappas, and H. S. Dhillon, "On the role of age of information in the Internet of Things," *IEEE Commun. Mag.*, vol. 57, no. 12, pp. 72–77, Dec. 2019.

[18] A. Kosta, N. Pappas, and V. Angelakis, "Age of information: A new concept, metric, and tool," *Found. Trends Netw.*, vol. 12, no. 3, pp. 162–259, Jun. 2017.

[19] B. T. Bacinoglu, Y. Sun, E. Uysal, and V. Mutlu, "Optimal status updating with a finite-battery energy harvesting source," *J. Commun. Netw.*, vol. 21, no. 3, pp. 280–294, Jun. 2019.

[20] C. Kam, S. Kompella, G. D. Nguyen, J. E. Wieselthier, and A. Ephremides, "On the age of information with packet deadlines," *IEEE Trans. Inf. Theory*, vol. 64, no. 9, pp. 6419–6428, Mar. 2018.

[21] I. Kadota, A. Sinha, E. Uysal-Biyikoglu, R. Singh, and E. Modiano, "Scheduling policies for minimizing age of information in broadcast wireless networks," *IEEE/ACM Trans. Netw.*, vol. 26, no. 6, pp. 2637–2650, Dec. 2018.

[22] R. D. Yates and S. K. Kaul, "The age of information: Real-time status updating by multiple sources," *IEEE Trans. Inf. Theory*, vol. 65, no. 3, pp. 1807–1827, Sep. 2018.

[23] Y. Inoue, H. Masuyama, T. Takine, and T. Tanaka, "A general formula for the stationary distribution of the age of information and its application to single-server queues," *IEEE Trans. Inf. Theory*, vol. 65, no. 12, pp. 8305–8324, Aug. 2019.

[24] J.-B. Seo and J. Choi, "On the outage probability of peak age-of-information for D/G/1 queuing systems," *IEEE Commun. Lett.*, vol. 23, no. 6, pp. 1021–1024, Apr. 2019.

[25] S. Leng and A. Yener, "Age of information minimization for an energy harvesting cognitive radio," *IEEE Trans. Cogn. Commun. Netw.*, vol. 5, no. 2, pp. 427–439, Jun. 2019.

[26] Y. Gu, H. Chen, C. Zhai, Y. Li, and B. Vucetic, "Minimizing age of information in cognitive radio-based IoT systems: Underlay or overlay?" *IEEE Internet Things J.*, vol. 6, no. 6, pp. 10273–10288, Aug. 2019.

[27] S. Hao and L. Duan, "Regulating competition in age of information under network externalities," *IEEE J. Sel. Areas Commun.*, vol. 38, no. 4, pp. 697–710, Apr. 2020.

[28] J. Wang, C. Jiang, Z. Han, Y. Ren, and L. Hanzo, "Internet of Vehicles: Sensing-aided transportation information collection and diffusion," *IEEE Trans. Veh. Technol.*, vol. 67, no. 5, pp. 3813–3825, May 2018.

[29] J. Wang, C. Jiang, H. Zhang, Y. Ren, K.-C. Chen, and L. Hanzo, "Thirty years of machine learning: The road to Pareto-optimal wireless networks," *IEEE Commun. Surveys Tuts.*, vol. 22, no. 3, pp. 1472–1514, 3rd Quart., 2020.

[30] M. A. Abd-Elmagid and H. S. Dhillon, "Average peak age-of-information minimization in UAV-assisted IoT networks," *IEEE Trans. Veh. Technol.*, vol. 68, no. 2, pp. 2003–2008, Dec. 2018.

[31] W. Li, L. Wang, and A. Fei, "Minimizing packet expiration loss with path planning in UAV-assisted data sensing," *IEEE Wireless Commun. Lett.*, vol. 8, no. 6, pp. 1520–1523, Dec. 2019.

[32] G. Han, X. Long, C. Zhu, M. Guizani, Y. Bi, and W. Zhang, "An AUV location prediction-based data collection scheme for underwater wireless sensor networks," *IEEE Trans. Veh. Technol.*, vol. 68, no. 6, pp. 6037–6049, Jun. 2019.

[33] C. Lin, G. Han, M. Guizani, Y. Bi, J. Du, and L. Shu, "An SDN architecture for AUV-based underwater wireless networks to enable cooperative underwater search," *IEEE Wireless Commun.*, vol. 27, no. 3, pp. 132–139, Jun. 2020.

[34] N. Wang and J. Wu, "Trajectory scheduling for timely data report in underwater wireless sensor networks," in *Proc. IEEE Global Commun. Conf. (GLOBECOM)*, San Diego, CA, USA, Dec. 2015, pp. 1–6.

[35] M. T. R. Khan, Y. Z. Jembre, S. H. Ahmed, J. Seo, and D. Kim, "Data freshness based AUV path planning for UWSN in the Internet of Underwater Things," in *Proc. IEEE Global Commun. Conf. (GLOBECOM)*, Waikoloa, HI, Feb. 2019, pp. 1–6.

[36] L. Brekhovskikh and Y. P. Lysanov, *Fundamentals of Ocean Acoustics*, vol. 116. Heidelberg, Germany: Springer, 2004.

[37] N. Morozs, W. Gorma, B. T. Henson, L. Shen, P. D. Mitchell, and Y. V. Zakharov, "Channel modeling for underwater acoustic network simulation," *IEEE Access*, vol. 8, pp. 136151–136175, 2020.

[38] M. Zorzi, P. Casari, N. Baldo, and A. F. Harris, "Energy-efficient routing schemes for underwater acoustic networks," *IEEE J. Sel. Areas Commun.*, vol. 26, no. 9, pp. 1754–1766, Nov. 2008.

[39] J. Liu, X. Wang, B. Bai, and H. Dai, "Age-optimal trajectory planning for UAV-assisted data collection," in *Proc. IEEE Conf. Comput. Commun. Workshops (INFOCOM WKSHPS)*, Honolulu, HI, USA, Apr. 2018, pp. 553–558.

[40] D. R. Morrison, S. H. Jacobson, J. J. Sauppe, and E. C. Sewell, "Branch-and-bound algorithms: A survey of recent advances in searching, branching, and pruning," *Discr. Optim.*, vol. 19, pp. 79–102, Feb. 2016.

[41] N. Tian and Z. G. Zhang, *Vacation Queueing Models: Theory and Applications*, vol. 93. New York, NY, USA: Springer, 2006.

Zhengru Fang (Graduate Student Member, IEEE) received the B.S. degree in electronics and information engineering from Huazhong University of Science and Technology, Wuhan, China, in 2019. He is currently pursuing the M.S. degree in electronics and communication engineering from Tsinghua University, Beijing, China.

His research interests lie in the area of Internet of Underwater Things and mobile-edge computing.

Jingjing Wang (Member, IEEE) received the B.S. degree (Highest Hons.) in electronic information engineering from Dalian University of Technology, Dalian, China, in 2014, and the Ph.D. degree (Highest Hons.) in information and communication engineering from Tsinghua University, Beijing, China, in 2019.

From 2017 to 2018, he visited the Next Generation Wireless Group chaired by Prof. L. Hanzo, University of Southampton, Southampton, U.K. He is currently a Postdoctoral Researcher with the Department of Electronic Engineering, Tsinghua University. His research interests include resource allocation and network association, learning theory aided modeling, analysis, and signal processing, as well as information diffusion theory for mobile wireless networks.

Dr. Wang was a recipient of the Best Journal Paper Award of IEEE ComSoc Technical Committee on Green Communications & Computing in 2018, and the Best Paper Award from IEEE ICC and IWCMC in 2019.

Chunxiao Jiang (Senior Member, IEEE) received the B.S. degree (Highest Hons.) from Beihang University, Beijing, China, in 2008, and the Ph.D. degree (Highest Hons.) in electronic engineering from Tsinghua University, Beijing, in 2013.

From 2011 to 2012, he visited the University of Maryland, College Park, MD, USA, as a joint Ph.D. supported by China Scholarship Council. From 2013 to 2016, he was a Postdoctoral Fellow with Tsinghua University, during which he visited the University of Maryland and University of Southampton, Southampton, U.K. Since July 2016, he has been an Assistant Professor with Tsinghua Space Center, Tsinghua University. His research interests include space networks and heterogeneous networks.

Dr. Jiang is a recipient of the Best Paper Award from IEEE GLOBECOM in 2013, the Best Student Paper Award from IEEE GlobalSIP in 2015, IEEE Communications Society Young Author Best Paper Award in 2017, the Best Paper Award IWCMC in 2017, and the Best Journal Paper Award of IEEE ComSoc Technical Committee on Communications Systems Integration and Modeling in 2018.

Qinyu Zhang (Senior Member, IEEE) received the bachelor's degree in communication engineering from Harbin Institute of Technology (HIT), Harbin, China, in 1994, and the Ph.D. degree in biomedical and electrical engineering from the University of Tokushima, Tokushima, Japan, in 2003.

From 1999 to 2003, he was an Assistant Professor with the University of Tokushima. From 2003 to 2005, he was an Associate Professor with Shenzhen Graduate School, HIT, where he was also the Founding Director of the Communication Engineering Research Center, School of Electronic and Information Engineering. Since 2005, he has been a Full Professor and the Dean of the EIE School, HIT, and also with the Network and Communication Research Center, Peng Cheng Laboratory, Shenzhen, China. His research interests include aerospace communications and networks, wireless communications and networks, cognitive radios, signal processing, and biomedical engineering.

Prof. Zhang received three scientific and technological awards from governments and received the National Science Fund for Distinguished Young Scholars, the Young and Middle-Aged Leading Scientist of China, and the Chinese New Century Excellent Talents in University. He was the TPC Co-Chair of the IEEE/CIC ICCC 15, the Symposium Co-Chair of the IEEE VTC 16 Spring, the Associate Chair of Finance of ICMMT 12, and the Symposium Co-Chair of CHINACOM 11. He was the Founding Chair of the IEEE Communications Society Shenzhen Chapter. He is on the Editorial Board of some academic journals, such as the *Journal on Communications*, the *KSII Transactions on Internet and Information Systems*, and *Science China: Information Sciences*. He has been a TPC Member of INFOCOM, ICC, GLOBECOM, WCNC, and other flagship conferences in communications.

Yong Ren (Senior Member, IEEE) received the B.S., M.S., and Ph.D. degrees in electronic engineering from Harbin Institute of Technology, Harbin, China, in 1984, 1987, and 1994, respectively.

He worked as a Postdoctoral Fellow with the Department of Electrical Engineering, Tsinghua University, Beijing, China, from 1995 to 1997, where he is currently a Full Professor with the Department of Electronic Engineering and serves as the Director of the Complexity Engineered Systems Lab, and also with the Network and Communication Research Center, Peng Cheng Laboratory, Shenzhen, China. He has authored or coauthored more than 400 technical papers in the area of computer network and mobile telecommunication networks. His current research interests include complex system theory and its applications to the optimization of the Internet, Internet of Things and ubiquitous network, cognitive networks, and cyber–physical systems.

Prof. Ren has served as a reviewer of more than 40 international journals or conferences.